JOURNAL OF MATERIALS SCIENCE 14 (1979) 1141–1151

Geometric probability approach to the examination of microcracking in plain concrete

P. STROEVEN
Stevin Laboratory, Department of Civil Engineering, Delft University of Technology, The Netherlands

The paper aims at connecting in a quantitative way the engineering behaviour of plain concrete subjected to uniaxial compression to the main features of microcracking. The selected structural level conceives the concrete as a two-phase material, the smallest structural dimensions of which could be measured in millimetres. It is shown that geometric probability theory provides the basis for an elegant and general framework for the quantification of microcracking, and yet the image analysis procedures described rely exclusively on simple counting operations. Crack length (in a plane) and particularly specific crack surface area in connection with the specific surface area of the grains reveals information with respect to the intensity of structural loosening in the various load stages. The minor influence of the loading level is demonstrated to be reflected also by the small degree of orientation of the cracks. A simple concept for spacing is developed. Application shows the growing order in the crack structure under increasing load. Finally, the average crack length is determined. Since the probability density of crack length in a plane was shown to be governed by a simple exponential function, the maximum crack length could be determined in an equally simple way.

Notation

$\bar{P}_L\ (=\bar{P}/L)$	Number of intersections of cracks in a section with a superimposed system of randomly distributed lines per unit of line length.
$P_L(\theta)$ $(P_L)_\perp = P_L(\theta = \pi/2)$ $(P_L)_\parallel = P_L(\theta = O)$	Number of intersections of cracks in a section with a line grid composed of straight parallel lines positioned in such a way that it successively encloses an angle θ, $\theta = \pi/2$ and $\theta = O$, respectively, with the axis of symetry.
$L_A\ (=L/A)$	Total crack length in a section per unit of area.
$(L_A)_{or}$	Oriented portion of L_A. Because of the assumption of linear orientation these cracks all run parallel to the axis of symmetry.
$S_V\ (=S/V)$	Total crack surface area per unit of volume.
$(S_V)_{or}$	Oriented portion of S_V, composed of cracks running parallel to the axis of symmetry.
$(S_V)_{TP}$	Total projected area of S_V onto a plane.
$V_V\ (=V/V)$	Volume fraction.
λ, Δ_2	Mean free spacing and average nearest neighbour distance in a plane, respectively.
$N_A\ (=N/A)$	Number of cracks in a section per unit of area.
$x, \hat{x}$	Crack length and maximum crack length, respectively.

$$\left.\begin{aligned}\omega_2 &= (L_A)_{or}/L_A \\ \omega_3 &= (S_V)_{or}/S_V\end{aligned}\right\} \quad \text{Degree of orientation.}$$

A bar over a symbol indicates an average value. In general, the division sign is omitted in stereological literature; the numerator refers to the crack system and the denominator to the sampling system.

1. Introduction

In order to understand the actual fracture behaviour or to interpret a mechanical test in terms of service behaviour, one has to leave the engineering level, where concrete is assumed to be homogeneous, isotropic, thus structureless, and to descend to the underlying microstructural level. In doing so, the process of structural loosening under increasing loads can be disentangled into local events.

The details and average characteristics of this process of disrupture have constituted the subjects of our studies for many years [1–4]. In addition, a methodological framework for structural analyses has been developed [1, 2, 5] and applied to solve various engineering and structural problems [6–8]. As for the latter, we have so far obtained relevant information with respect to the operating crack mechanisms on the microstructural level [1, 9].

In this paper we will focus on the dependence of the average features of the process of structural loosening, as revealed on an engineering level, on the average structural changes due to microcracking. This way of tackling the problem offers a structural interpretation of volumetric changes. More generally, insight is acquired in the micromechanical behaviour of concrete under mechanical loading.

A study of the microcracking phenomenon in concrete specimens has to be based upon a quantitative image analysis of sections taken from these specimens. The information available, therefore, is of a two-dimensional character. As a consequence, one should look for relationships in geometric probability theory which could facilitate a three-dimensional interpretation of the data. The very part of science that deals with the formulation of these statistico-geometrical relationships is called stereology. Stereology is defined as a system of methods to obtain information about three-dimensional structures from two-dimensional images (sections or projections).

In order to represent engineering (i.e. average microstructural) features the section or projection should be of representative size. In dealing with a macroscopically heterogeneous material like concrete the so called representative volume element (RVE) is an imaginary unit of macroscopical size representing to a defined and arbitrary probability the heterogeneity of the material. In the same way we can define a representative area element (RAE) for quantitative image analysis [1, 5].

Crack "initiation", as a structure-sensitive property, will be governed by the complete configuration of grains (gravel, sand) in concrete. This is most pronounced in low-stressed specimens, where the density of the cracks is relatively low. Since the linear dimensions of an RAE for configuration homogeneity surpass those for composition homogeneity by, roughly, one order of magnitude [5, 6], this may lead to very large specimens or numerous "identical" specimens, when the cracking phenomenon is surveyed. Fortunately, virgin specimens have long left behind this stage of crack initiation under conditions of moderate temperature and humidity, because of rather intense shrinkage cracking, causing the influence of the load intensity on the crack structure over the complete loading range to be strongly decreased [10, 11].

The structural level, selected for our experiments, conceived the concrete as a two-(or multi-) phase material, the smallest structural dimensions of which still could be measured in millimeters. This implies that only grains or cracks having linear dimensions in excess of 1 to 2 mm were considered, which defines the level of the microstructure taken into consideration. The stereological approach to be described will supply average characteristics of microcracking. It will reflect the mean features of local cracking behaviour, i.e. crack formation around inclusions embedded in a matrix. Since information on this very topic had been obtained by microscopical observations in previously performed tests [1, 3], the data produced by the image analysis process could also be evaluated in this sense.

2. Historical background

Although stereology is a recently established discipline [13], stereological techniques for image analysis are based upon coverage techniques which

date back as far as two centuries. Nevertheless, quantitative image analysis started as an empirical technique in petrography halfway through the previous century [14]. Moreover, despite a widespread use of various quantitative image analysis techniques in metallurgy and biosciences, it was not until the end of the Second World War that Saltikov presented his directed and random secants techniques applied in our investigations. These latter techniques are superior compared to other techniques in vogue at that time, in the sense that they are far less time-consuming. Saltikov's solution is quite similar, however, to the one given by Buffon in 1776 for the "needle problem" [1, 15, 16].

We have previously reported [1] further details of the historical background. For applications of stereology in the field of concrete technology, the most common one of which is the determination of the pore (size) distribution, see [1, 6, 7].

3. Stereological framework for the examination of microcracking

Microcracking manifests itself in sections as lineal features in a plane. The methods proposed by Saltikov are based on coverage of the sample plane by a line grid. Either a uniformly spaced grid of straight lines can be used in the case of the directed secants technique, or a randomly positioned and oriented set of lineal elements can be superimposed on the crack pattern. Both methods ask only for a count of the number of intersections, P, with the lineal features. Dividing through by the total line length, L, will yield $P/L = P_L$ (Fig. 1).

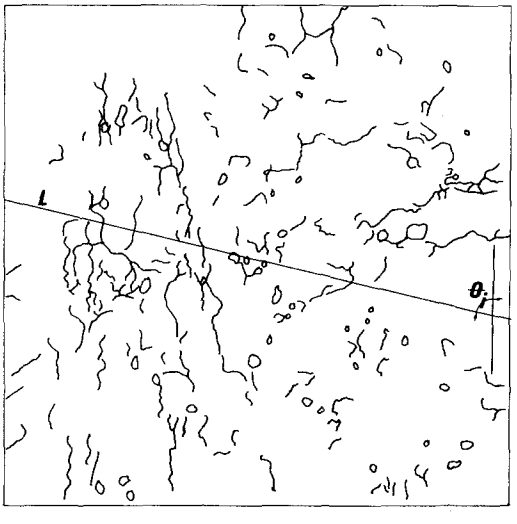

Figure 1 Application of the method of directed secants.

Many of the interesting three-dimensional characteristics of the structure of the material (in this case the cracks in concrete) can be derived from these primary data as demonstrated earlier [1, 2, 6].

A two-dimensional analysis of the crack pattern – the normal approach in concrete technology [17] – can be based upon the relationships

$$L_A = \frac{\pi}{2} \bar{P}_L \tag{1}$$

where $\bar{P}_L$, as defined above, is determined by means of a system of random secants, and L_A is the total crack length per unit of sampled area.

$$\omega_2 = (L_A)_{or}/L_A = \{(P_L)_\perp - (P_L)_\parallel\}/ \{(P_L)_\perp + 0.571\,(P_L)_\parallel\} \tag{2}$$

in which $(L_A)_{or}$ equals the oriented portion of L_A and ω_2 is the degree of orientation.

According to Equation 2 ω_2 can be calculated from two intersection counts with a line array perpendicular and parallel to the symmetry (orientation) axis, respectively.

Repeating the procedure for a number of successive values of θ, representing the angle enclosed by the axis of the system of directed secants and a reference axis, will yield $P_L(\theta)$ data. This information can be used to construct a polar figure, also termed the rose of the number of intersections, that reflects the actual crack orientation distribution in the sampled plane (see Fig. 7).

In conclusion it can be stated that L_A, on the one side, and $P_L(\theta)$ and ω_2, on the other, can be used to analyse inhomogeneity (or segregation) and anisometry (causing anisotropy) in the sample plane, respectively.

A framework for a three-dimensional analysis can similarly be developed. A measure for the specific surface area of the cracks, S_V, is obtained by extending the averaging procedure of the intercept count over two independent spatial angles $\{\theta, \varphi\}$. Hence

$$S_V = 2\bar{P}_L \tag{3}$$

where the bar indicates a volume average.

In order to keep the procedure manageable it is necessary (i.e. to avoid preparing a random set of sections) to assume the partially oriented crack system to manifest a linear orientation. This implies that the real system can be separated in a random and a completely ordered portion. This

type of order is such that all elements are oriented in one direction. In this case the analysis can be limited to a single section of a cylindrical (or, approximately, a prismatic) specimen, parallel to the axis of symmetry. As was shown previously [1, 6], one can make use of the relationships

$$S_V = 0.429\,(P_L)_{\parallel} + 1.571\,(P_L)_{\perp} \quad (4)$$

$$\omega_3 = (S_V)_{or}/S_V = \{(P_L)_{\perp} - (P_L)_{\parallel}\}/\{(P_L)_{\perp} + 0.273\,(P_L)_{\parallel}\} \quad (5)$$

in which $(S_V)_{or}$ represents the oriented portion of S_V.

It can be concluded that a complete three-dimensional analysis of inhomogeneity and anisometry of the crack structure in a concrete specimen can be performed on the basis of two-dimensional observations in a single axial section. These observations simply consist of counts of the number of intersections corresponding to two predescribed positions of a uniformly spaced linear array

An investigation of the spatial orientation distribution of the cracks of equal simplicity as compared to the two-dimensional case is not possible. It can be shown that $P_L(\theta)$ constitutes only a biased estimate for it [18]. Yet, starting from the two-dimensional rose, reflecting the crack orientation distribution in an axial section, Hilliard [19] described a more complicated mathematical procedure which, finally, yields a system of simultaneous equations from the solution of which the spatial distribution can be derived. For details one is referred, however, to the original literature [20–22].

4. Stereological spacing concept

Regardless of size, shape and distribution, the mean free spacing of dispersed discrete objects will be described by [1, 23]

$$\lambda = 4(1 - V_V)/S_V. \quad (6)$$

Assuming the volume fraction $V_V \ll 1$ we find upon substitution of Equation 3

$$\lambda = 2/\bar{P}_L. \quad (7)$$

λ constitutes a real three-dimensional spacing parameter (although it is the same in a random section), defining the average unobstructed surface-to-surface distance between particles (in this case, the crack surfaces). Equation 7 facilitates determination of the crack spacing by performing a counting operation in a single section. In that case Equation 4 instead of 3 is substituted in Equation 7.

When cracks having a specific surface area S_V are randomly distributed, it can be shown that 50% of S_V is oriented in the direction of an arbitrary plane [6]. Hence

$$(S_V)_{TP} = 0.5\,S_V. \quad (8)$$

$(S_V)_{TP}$ can also be conceived as the total projection of S_V on the plane in question. The corresponding mean free spacing of this part of the cracks is, of course, twice as large as that of the random system.

In addition to λ, which can be understood to characterize the overall composition, one can use the average nearest neighbour distance in a plane Δ_2, which is more closely related to configuration. It can be demonstrated that [1, 11]

$$\Delta_2 = 0.5/N_A^{1/2} \quad (9)$$

N_A being the number of features (cracks) per unit of sampled area. Δ_2 presents a measure for the average centre-to-centre distance of randomly dispersed nearest neighbours in a plane. Application only requires counting the number of cracks in a section.

For partly ordered systems, the coefficient 0.5 in Equation 12 has to be increased [1, 24].

5. Crack size analysis

Unfortunately, a three-dimensional size concept as simple as the spacing concept cannot be developed. First, one should construct a model from which the relation between the observed crack length, x, in a section and the spatial crack size, r, of the crack surfaces cut by the section plane can be obtained. Secondly, r should be connected with R, representing the size of the crack surfaces in the specimen. The latter problem can be tackled by applying the theory of statistics of extremes. The solution of the first sampling problem, however, is limited to relatively simple crack shapes, e.g. discs. For this case the author has developed a three-dimensional size concept [25].

In the present paper we will follow, however, the common way in concrete technology, i.e. a two-dimensional size analysis. The average crack length, $\bar{x}$, is obviously given by

$$\bar{x} = L_A/N_A. \quad (10)$$

Following Fisher and Hollomon [26] one can

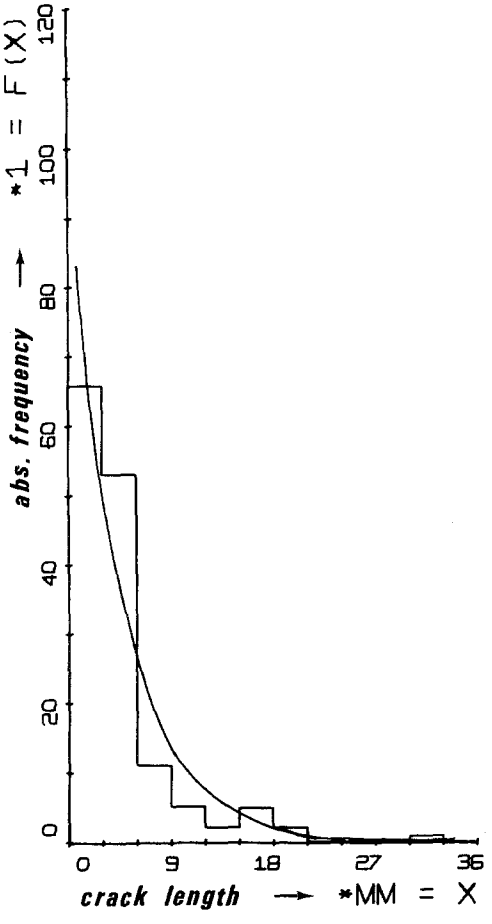

Figure 2 Two-dimensional crack size distribution for an axial section of a prismatic specimen subjected to uniaxial compression up to load level 9 (see Fig. 4). The histogram reflects the measurements, while the continuous curve corresponds to the theoretical prediction due to Equation 11.

assume the size distribution of the cracks to be described by

$$\Phi(x) = \exp(-x/\bar{x})/\bar{x}. \tag{11}$$

By means of an automatic scanner (Quantimet 720) we have verified Equation 11 for the test series to be described. It is demonstrated by Fig. 2 that the probability density function $\Phi(x)$ constitutes a suitable prediction for the actual two-dimensional crack size distribution as revealed by sections of uniaxially compressed specimens.

The maximum crack size, $\hat{x}$, corresponding to selected confidence limits for $\bar{x}$ follows through simple integration of Equation 11. Hence

$$\hat{x}(95\%) = 3.0\,\bar{x}$$
$$\hat{x}(99\%) = 4.7\,\bar{x}$$
$$\hat{x}(99.95\%) = 7.7\,\bar{x}.$$

The last confidence limit roughly corresponds to the situation in our experiments where only the size of a single crack in the section area will surpass this limit.

To solve the crack size problem two separate counting procedures (for P_L and N_A) are sufficient to generate the relevant information.

6. Accuracy

For the two methods involved, the one based on an intersection count (P) the other on a profile count (N), it is possible to calculate the number of counts necessary to achieve a given accuracy in the surface fraction (S_V), the specific crack length (L_A), the spacing factors (Δ_2 and λ) and the size parameter ($\bar{x}$). For that purpose it is assumed that both cases are governed by a Poisson field. For non-contiguous particles occupying a small volume fraction (say, $< 15\%$) Hilliard gives as an estimate for the relative standard deviation of the specific surface area obtained by sampling with a line grid [27]

$$\sigma(S_V)/\bar{S}_V = (2/P)^{1/2}, \tag{13}$$

in which P is the total number of intersections.

On substitution of Equations 1 and 3 into Equation 13 it follows that

$$\sigma(L_A)/\bar{L}_A = \left(\frac{8}{\pi}/P\right)^{1/2}. \tag{14}$$

It should be mentioned that Equations 13 and 14 are only valid when the number of intersections does not exceed the number of profiles (cracks).

To attain a coefficient of variation of 10% for the specific crack length, it can be demonstrated that a sample area of about 100 mm x 100 mm will be sufficient in the case of the crack density data met in our experiments.

Knowing the variance in the values of S_V and L_A it is possible to estimate the accuracy with which the spacing and size parameters can be obtained that are connected with either S_V or L_A. The relative standard deviation of the profile density is obviously given by

$$\sigma(N_A)/\bar{N}_A = N^{-1/2}. \tag{15}$$

which yields for Δ_2

$$\sigma(\Delta_2)/\bar{\Delta}_2 = 0.5\,N^{-1/2}. \tag{16}$$

7. Results

The primary purpose of the experimental survey is to illustrate the applicability of the methodolo-

gical and theoretical concept for the solution of technological problems. On the other hand, the investigation of the crack development process was undertaken to look for the characteristic features of microcracking which underly the engineering behaviour. In the uniaxial compression tests we have particularly tried to interpret the different stages in the macromechanical behaviour under increasing loads in terms of those features which obviously were of dominant influence. From previous tests (including microscopical [1, 28] as well as holographic interferometrical observations [3, 4]) we were able to construct a model for local crack formation around inclusions (gravel and sand grains). This facilitated a bridge over the dimensional gap between the engineering behaviour and the local fracture mechanisms successively in action under increasing loads. The results presented concern a study of the cracking pheno-

Figure 3 The pattern of surface cracking is visualized by means of the filtered particle method [28–30]. The surface crack pattern of a specimen loaded up to level 9 is shown at the left. Further, the cracks visible with the unaided eye are copied. Two of the patterns are presented below, the left one corresponding to the zero-loading stage and the right one to loading stage 9, at which the test was stopped (see Fig. 4). The uniaxial compressive stress equalled 32 N mm^{-2} at that stage.

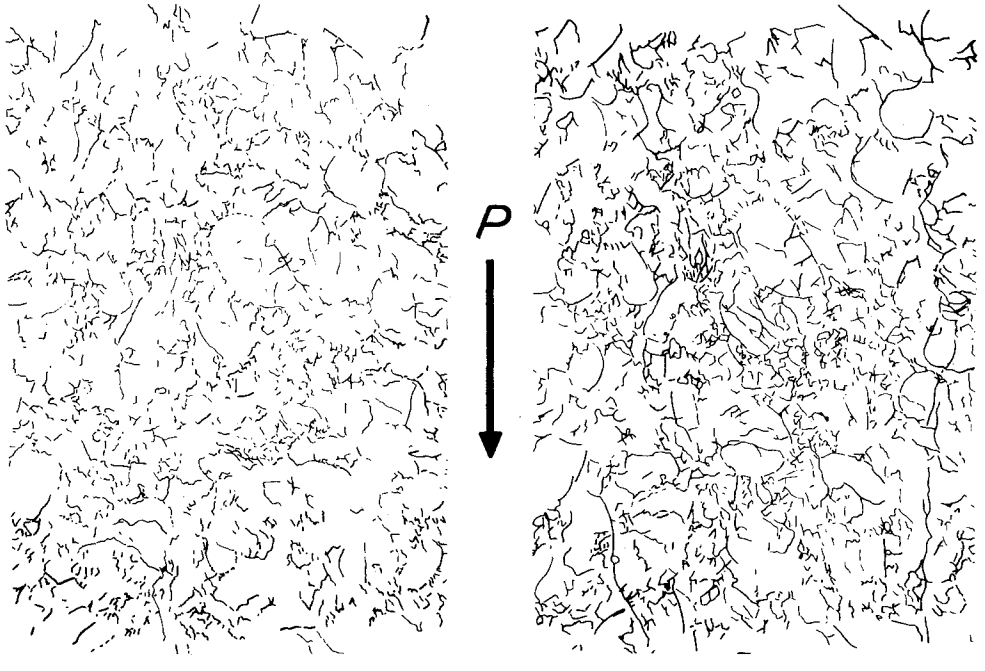

TABLE I Aggregate grading of concrete

Sieve opening (mm)	Sieve rest (%)
23	–
11.2	32
5.6	28
2.8	18
1.4	10
0.6	6
0.3	4
0.15	1
< 0.15	1
Total	100

menon in three similar concrete prisms (110 mm × 110 mm × 500 mm) subjected to uniaxial compressive loadings. The aggregate grading is shown in Table I. The PC-content (type A) was 375 kg m^{-3} and a W/C ratio of 0.48 was used. The specimens were wet-cured for 1 month and subjected for about 2 months to the test conditions (50% r.h., 20° C).

Two of the tests were load-controlled, the third one being displacement controlled. The data to be presented refer, however, exclusively to the latter test condition. The load or displacement was adjusted to the required level and maintained for some time to allow the fluorescent dye to penetrate into the cracks and to dry (Fig. 3). Finally, the load was removed and the specimen transported to the photographic apparatus, where the crack patterns were recorded. In this way, successively, the various load stages were scanned. The relevant axial stress–strain cycles and the levels selected for further structural elaborations are shown in Fig. 4. The three axial stress–transverse strain cycles, corresponding to the selected levels 6, 8 and 9, are shown if Fig. 5. Quite obviously the deformations in the transverse direction reflect two different development processes in the internal cracking, a transition "point" being roughly located at 26 N mm^{-2}. Thus, the selected load levels represent one state below and two beyond this point. More specifically, level 8 is taken close to the maximum in the stress–strain curve, while level 9 is situated well over this "top".

The crack patterns have been copied manually – the result of which is shown at the bottom of Fig. 3 – and analysed by the described stereological techniques. In addition, an alternative method was applied. This method consists of superimposing an ellipse-like curve in a prescribed position on the pattern of cracks [20, 21]. A single count of the number of intersections suffices. Dividing through by twice the length of the minor axis yields a result that can be compared directly with that of Equation 4.

The bottom part of Fig. 5 shows the development of the crack surface area per unit of volume under increasing load. The crack pattern present in the virgin specimen obviously dominates the load-induced portion. The increase in the specific crack surface area over the complete loading range only amounts to 26.2%. A minor part of it contributes to the partial orientation as is demonstrated by Fig. 7. In addition, it is shown that a two-dimensional interpretation of the sections can also reveal sufficient information to characterize the process of structural loosening. The graph for L_A as a function of the axial stress even

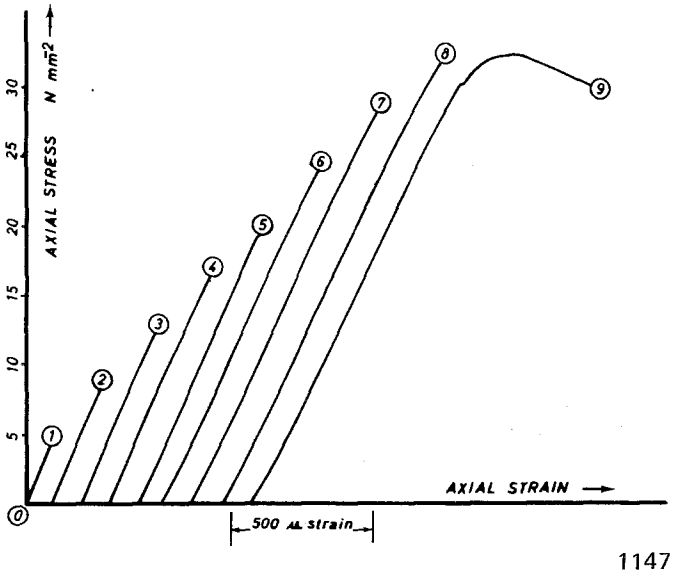

Figure 4 The stress–strain regimes in uniaxial compression to which a prismatic specimen is subjected in a displacement-controlled bench. The crack patterns have been analysed in the indicated positions (0 to 9). The results of 0, 6, 8 and 9 have been used throughout this paper.

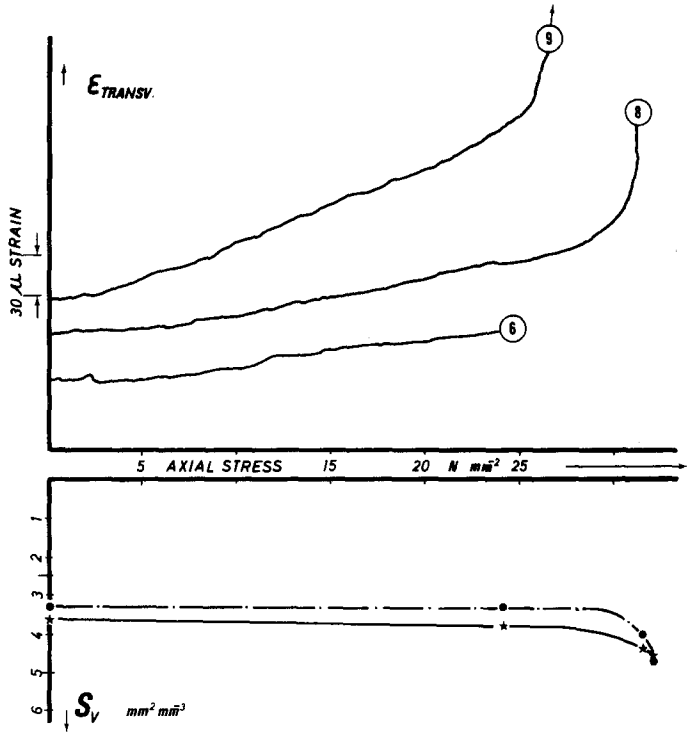

Figure 5 The development of the transverse strains in a uniaxially compressed prism, corresponding to the load cycles 6, 8, and 9. Further, the specific crack surface area, S_V, is shown as a function of the axial stress • ·—·— • $S_V = 0.429\,(P_L)_{\parallel} + 1.571\,(P_L)_{\perp}$ ★——★ $S_V = 2P_L$ using an ellipse-like line system [20–22].

showed a slightly more pronounced increase beyond discontinuity as compared to the path of the S_V curve. An increase of 29% in crack length between load stages 6 and 8 could be observed [12].

The information stored in the roses-of-the-number-of-intersections, corresponding to the crack distribution in a plane, $P_L(\theta)$, reflects the acting mechanisms and the average features of crack development (degree and direction of partial orientation). Fig. 6 illustrates that the load-induced portion of the crack surface area per unit of volume, ΔS_V, is closely connected with the volumetric changes on engineering level. Phenomenological behaviour on macrolevel is thus directly related to the average structural changes.

Rupture can now be interpreted in structural terms. A small but gradual, though discontinuous, rising of crack length and number is observed in the first stage of loading. During the second stage

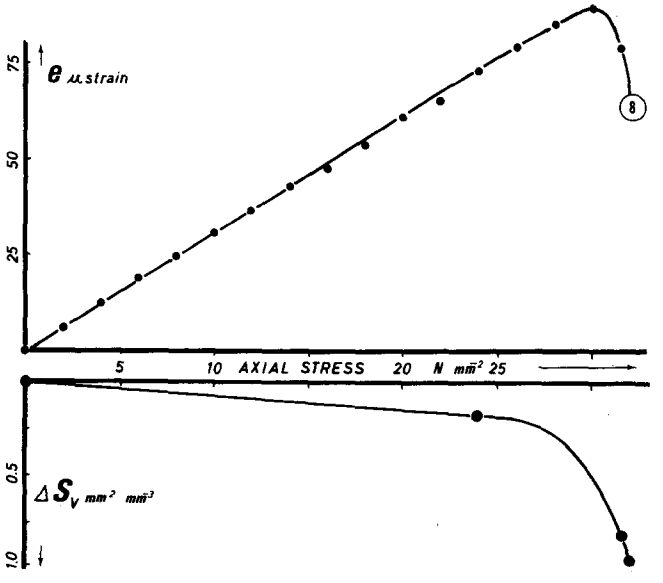

Figure 6 The mean normal strain, $e = (\epsilon_x + \epsilon_y + \epsilon_z)/3$, corresponding to load cycle 8, is shown in its dependence on the applied axial stress. At the bottom, the accompanying increase beyond discontinuity in the internal specific crack surface area, ΔS_V, is clearly demonstrated.

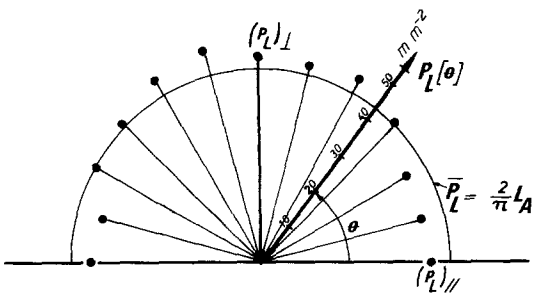

Figure 7 The rose-of-the-number-of-intersections, $P_L(\theta)$, corresponding to the surface crack pattern of the specimen loaded up to level 9. Cracking in the axial, loading, direction can be observed. The two- and three-dimensional values of the degree of orientation amount to 10.4% (ω_2) and 12.5% (ω_3), respectively.

the dominating mechanism consists in joining of cracks. This facilitates an increase in crack opening, however, producing only moderate increments in S_V values and even a final decrease in N_A, the number of cracks (in a plane). As a consequence, on the engineering level macrocracks are being initiated which by subsequent propagation finally cause the specimen to break down under the applied load.

All results are influenced, of course, by the degree of magnification. In our experiments we have taken into consideration only cracks in excess of about 1 mm long, which defines the level of the microstructure. Comparing these results with those obtained in similar experiments described in [1] it becomes obvious that the higher the magnification during the procedure of copying the cracks, the less pronounced is the oriented portion of the crack structure induced by the external loading. This is confirmed by results of experiments performed by the author, in which the effect of the direction of pouring and vibration upon the orientation distribution of the cracks was studied (see Fig. 11 in [5] or Fig. 2 in [28]). It was found, for example, that the degree of orientation, ω, was increased when the smaller cracks, present through the complete loading range, were omitted from the analysis.

8. Discussion

The relationship between the engineering behaviour, reflected in a quantitative way by the graph of the mean normal strain (Fig. 6) and microcracking can be provided with a further quantitative base by expressing the process of disrupture in terms of debonding. The degree of debonding of the gravel and sand grains is approximated by the ratio of the specific surface areas of the cracks and the sand and gravel grains at the same level of the microstructure. The total surface area of a mixture of spheres according to Popovics is given by [31]

$$S = b \sum_{i=1,2\ldots}^{n} \frac{R_i}{d_i} \qquad (17)$$

where R_i is the weight fraction on a sieve with opening d_i. For smooth spheres $b = 0.06$.

We have accounted for deviations of the grains from the spherical shape by assuming them to be spheroids. Minimum and maximum dimensions were measured for a set of grains out of each sieve rest. A correction factor for the total surface area as given by Equation 17 was calculated in this way. The contribution of the larger grains ($1\,\text{mm} \leqslant d \leqslant 1.4\,\text{mm}$) contained by the sieve rest on the sieve with openings 0.6 mm was not taken into consideration. In doing so, the data collected in Table II were obtained.

A comparison of these results demonstrates, again, the moderate rise in the degree of "debonding". Moreover, the crack mechanism of joining contributes to the creation of matrix cracks particularly under higher loads, thus even diminishing the tendency shown in Table II. A more precise value for the degree of debonding can, of course, be determined by optically distinguishing interface cracks from matrix cracks (see Shah and Slate [32]), a procedure which will not impose any additional problem in the stereological analysis. With respect to crack spacing,

TABLE II Degree of "debonding" or structural loosening

Load cycle	Cracks ($x > 1\,\text{mm}$) $(S_V)_c(\text{mm}^{-1})$	Grains ($d > 1.4\,\text{mm}$) $(S_V)_g(\text{mm}^{-1})$	$\frac{100(S_V)_c}{2(S_V)_g}$ (%)
0	0.562	0.950	29.6
6	0.652	0.950	34.3
8	0.772	0.950	40.7
9	0.903	0.950	47.6

TABLE III The average nearest neighbour distance in a plane Δ_2, the mean free spacing λ, the average length $\bar{x}$ and the maximum length, $\hat{x}$, of cracks, respectively

Load	λ(mm)	Δ_2 (mm)	$\bar{x}$(mm)	$\hat{x}$(99.95%) (mm)
0	7.1	1.45	1.77	13.6
6	6.1	1.60	2.05	15.8
8	5.2	1.70	3.40	26.2
9	4.4	1.65	3.83	28.7

the successive application of Equations 10 and 12 yields the results collected in Table III.

The increased size of the cracks with rising load calculated by means of Equations 10 to 12 and also shown in Table III causes the number of free distances to be diminished. The distances to the more remote neighbours are, in particular, obstructed. As a consequence λ is reduced during the crack development process. On the contrary, the joining of nearest neighbours, by which N_A is diminished, causes the distance between neighbouring cracks to be slightly increased. As a result, the crack pattern becomes more homogeneous.

From the crack size distribution function of load cycle 9, shown in Fig. 2, it follows that the number of crack sections having a length of 19 mm or more (being about the average grain size of the sieve rest on the sieve with the largest opening) is about 1.8% of the total number of cracks. The major part of these cracks can be expected to run in the direction of loading. The average nearest neighbour distance of the centres of these crack sections in a transverse plane, therefore, can be calculated to equal 13 mm, approximately. On the other hand, the mean free spacing will be about 21 mm. This value can be calculated on the basis of the reasoning behind Equation 20 and accounting for a different tangent height for the oriented cracks. The relatively small ratio of Δ_2 and λ points towards a still more uniform distribution of this portion of the cracks. Moreover, these results roughly confirm the experimental finding that the sub-macrocracks under relatively high uni-axial compressive loadings run parallel to the loading direction at a distance corresponding to the maximum grain size [33].

9. Conclusions

The geometric probability approach to describe microstructural characteristics suits interpretation of the process of disrupture of plain concrete specimens subjected to loading in terms of structural loosening, i.e. micro-fissuration. The complete image analysis procedures described rely exclusively on counting operations. The approach shares generality and simplicity. As such, the stereological framework can facilitate powerful tools to help solving structural problems.

References

1. P. STROEVEN, Ph. D. Thesis, Delft (1973).
2. *Idem,* Proceedings RILEM/IUPAC Symposium on Pore Structure and Properties of Materials (Academia, Prague, 1973/74) p. C 529.
3. P. STROEVEN and H. M. DE HAAS, Proceedings RILEM Symposium: New Developments in Non-Destructive Testing on Non-Metallic Materials (Constanza, Romania, V2, 1974) p. 19.
4. H. M. DE HAAS and P. STROEVEN, 10th Annual Conference BSSM "Strain Measurement and Analysis as an Aid to Design", Warwick (1974) Stevin Rep. 1–75–1, Delft (1975).
5. P. STROEVEN, Proceedings of the Symposium on Quantitative Analysis of Microstructures, Leoben, Practical Metallography Special Issue 5 (Riederer Verlag, Stuttgart, 1975) p. 291.
6. *Idem,* Proceedings of the Fourth International Congress for Stereology, Gaithersburg, (1975) p. 281, *J. Microsc.* **107** (1976) 313.
7. *Idem,* Proceedings RILEM Symposium on Fresh Concrete, Leeds, Vols. 1 to 3 (1973) papers paginated separately.
8. *Idem, J. Microsc.* **111** (1977) 283.
9. H. W. REINHARDT, P. STROEVEN, J. A. DEN UIJL, T. R. KOOISTRA, and J. H. A. M. VRENCKEN, *Bet. Fertigteil-Technik* **9** (1978) 498.
10. S. P. SHAH and G. WINTER *J. ACI* **63** (1966) 925, ACI publ. Sp 20 (1968) p.5.
11. J. GURLAND, "Quantitative Microscopy", edited by F. N. Rhines and R. T. de Hoff (McGraw-Hill, New York, 1968) p. 279.
12. P. STROEVEN, Proceedings of the Conference on Influence of volume change on the design and technology of modern building materials, Karlovy Vary (1975).
13. H. ELIAS, Proceedings of the Fourth International congress on Stereology, Gaithersburg (1975) NBS Spec. Publ. 431 (1976) p. VII.
14. F. CHAYES, "Petrographic modal analysis" (Wiley, New York, 1956).
15. S. A. SALTIKOV, "Stereometrische Metallographie", VEB Deutschen Verlag für Grundstoffenindustrie, Leipzig (1976) (translated from Russian).
16. E. E. UNDERWOOD, "Quantitative Microscopy", edited by R. T. De Hoff and F. N. Rhines (McGraw-Hill, New York, 1968) p. 78.
17. E. W. BENNET and N. K. RAJU, Proceedings of the Southampton Civil Engineering Materials Conference on Structure, Solid Mechanics and Engineering Design, edited by M. Te'eni (Wiley, London, New York, Sydney, Toronto, 1971) p. 86.
18. E. M. PHILOESKY and J. E. HILLIARD *Quart. Appl. Math.* **27** (1969) 79.
19. J. E. HILLIARD, *Trans. Met. Soc. AIME* **224** (1962) 1201.
20. E. M. PHILOFSKY, M.Sc. Thesis, Northwestern University, Evanston, Illinois (1966).
21. J. E. HILLIARD, Proceedings of the Second International Congress for Stereology, edited by H. Elias (Springer Verlag, New York, 1967) p. 211.
22. *Idem,* "Quantitative Microscopy" (McGraw-Hill, New York, 1968) p. 45.
23. E. E. UNDERWOOD, "Quantitative Microscopy" (McGraw-Hill, New York, 1968) p. 77.

24. J. E. HILLIARD, Proceedings of the International Conference, Haifa, edited by D. G. Brandon and A. Rosen (Israel University Press, Jerusalem, 1969) p. 3.
25. P. STROEVEN, Proceedings of the Second International Conference on Mechanical Behaviour of Materials, Boston (1976) p. 1675.
26. R. A. FISHER and J. H. HOLLOMON, Inst. Min. Metall. Eng., Techn. publ. no. 2218, August (1947) p. 1.
27. J. E. HILLIARD, Proceedings of the Fourth International Congress for Stereology, Gaithersburg (1975) NBS Spec. Publ. 431 (1976) p. 59.
28. P. STROEVEN, "Wlasności mechaniczne i struktura kompozytów betonowych", Ossolineum (1974) p. 367.
29. J. A. FORRESTER, Proceedings of the International Conference on The Structure of Concrete, London, edited by A. E. Brooks and K. Newman, (Cement and Concrete Association, 1968) p. 157.
30. S. I. DIAZ and H. K. HILSDORF, Civ. Eng. Studies, Struct. Res. Series no. 382 (University of Illinois, Urbana, 1971).
31. S. POPOVICS, *Mag. Concr. Res.* **57** (1966) 131.
32. S. P. SHAH and F. O. SLATE, Proceedings of the International Conference on The Structure of Concrete, edited by A. E. Brooks and K. Newman, (Cement and Concrete Association, 1968) p. 82.
33. L. J. M. NELISSEN, *Heron* **18** (1972) 1.

Received 14 July and accepted 6 September 1978.